

Merging of Unequal Mass Binary Black Holes in Non-Axisymmetric Galactic Nuclei

PETER BERCIK,^{1,2,3} MANUEL ARCA SEDDA,² MARGARYTA SOBOLENKO,³ MARINA ISHCHENKO,³ AND RAINER SPURZEM^{1,2}

¹*National Astronomical Observatories and Key Laboratory of Computational Astrophysics, Chinese Academy of Sciences, 20A Datun Rd., Chaoyang District, Beijing 100101, China*

²*Astronomisches Rechen Institut - Zentrum für Astronomie der Universität Heidelberg, Mönchhofstrasse 12-14, D-69120 Heidelberg, Germany*

³*Main Astronomical Observatory, National Academy of Sciences of Ukraine, 27 Akademika Zabolotnoho St., 03143 Kyiv, Ukraine*

(Received June 24, 2020; Revised June 24, 2020; Accepted August 12, 2020)

Submitted to ApJ

ABSTRACT

In this work we study the stellar-dynamical hardening of unequal mass supermassive black hole (SMBH) binaries in the central regions of galactic nuclei. We present a comprehensive set of direct N-body simulations of the problem, varying both the total mass and the mass ratio of the SMBH binary (SMBHB). Simulations are carried out with the φ -GPU N-body code, which enabled us to fully exploit supercomputers equipped with graphic processing units (GPUs). We adopt initial axisymmetric, rotating models, aimed at reproducing the properties of a galactic nucleus emerging from a galaxy merger event, containing two SMBHs initially unbound. We find no "final-pc problem", as our SMBHs tend to pair and shrink without showing significant signs of stalling. This confirms earlier results and extends them to large particle numbers and for rotating systems. We find that the SMBHB hardening depends on the binary reduced mass ratio via a single parameter function. Our results suggest that SMBHB at high redshifts are expected to merge with a factor of ~ 3 more efficiently, thus can significantly affecting the population of SMBHs potentially detectable as gravitational wave sources.

Keywords: black holes – binary black holes — galactic nuclei – stellar dynamics

1. INTRODUCTION

According to the hierarchical structure formation scenario in the Λ Cold Dark Matter (Λ CDM) paradigm, bright massive galaxies are supposed to form through mergers and accretion of smaller galaxies. SMBHs are commonly observed at the centers of most galaxies, and their mass correlates with several properties of their host galaxy, such as bulge mass (Ho & Kim 2014) or central velocity dispersion (see e.g., Gültekin et al. 2009). Therefore, if the majority of galaxies harbor an SMBH in their centers, SMBHB should represent an unavoidable outcome of the hierarchical formation scenario (Begelman et al. 1980). Several works attempted at detecting SMBHB in galactic nuclei, for instance chasing special patterns in radio lobes, jets, or quasi-periodic electromagnetic emission in their light curves (Komossa 2006). In some cases, these techniques permitted to constrain orbital properties an estimate the bi-

nary parameters. Two examples are 0402+379, a galaxy containing an SMBH pair candidate with total mass $\sim 10^8 M_{\odot}$, identified via radio observations achieved with the very long baseline interferometer (VLBI, see e.g. Rodriguez et al. 2006), or OJ287, an SMBHB candidate detected via quasi-periodic outbursts for which it has been possible to model the binary separation (~ 0.05 pc), eccentricity (~ 0.6) and spin (modeled taking into account even the spin-orbit interaction, see Valtonen 2007; Valtonen et al. 2010a,b).

The relativistic in-spiral and final coalescence driven by gravitational wave (GW) emission makes SMBHB among the strongest sources to be measured with future GW space satellite missions, like the Laser Interferometer Space Antenna (LISA) (Gong et al. 2011; Amaro-Seoane et al. 2013, 2017), or the TianQin (Luo et al. 2016) and Taiji (Ruan et al. 2018) space detectors. It is therefore of paramount importance to understand the astrophysical processes that drive SMBHBs from the unbound, pre-merger state, into the relativistic regime and their associated efficiency. This information can be used to place robust, and physically motivated,

constraints on the merger rate of these GW sources and provide a test-bed for GW signal templates to be compared with future observations.

However, the large amount of existing works focused on full numerical simulations of SMBHs pairing and evolution did not fully cover all the important parameters space yet. In particular, within the hierarchical galaxy formation scenario the range of mass ratios in galaxy mergers can hugely vary from 1:1 (major mergers) to 1:3, down to minor mergers, i.e. with mass ratios even below 1:10 (cfr. e.g. Naab et al. 2006, 2009). Given the correlations between galaxies and SMBHs masses, it is thus expected that also SMBHBs should form with a wide range of mass ratios. However, the majority of numerical studies based on N-body models focused mostly on nearly equal mass binaries. Moreover, the galactic nucleus produced in a galaxy merger event is expected to preserve a non-negligible rotation due to the global angular momentum conservation. The collective motion of stars affected by the rotation of the galactic nucleus can have a non-trivial effect onto the SMBHB evolution. In this paper, we expand the simulations presented in Berczik et al. (2006) by exploring a wider range of mass ratios, 0.01–1, and taking into account also the rotating nuclei.

Furthermore, the new simulations are based on our improved φ -GPU N-body code (Berczik et al. 2013b) that implements General Relativity effects in the form of post-Newtonian corrections to the equations of motion (Sobolenko et al. 2017; Khan et al. 2016). This will enable us to follow the SMBH binary evolution as the result of the simultaneous action of stellar hardening and GW emission all the way to final coalescence, and to model the GW signal during the final inspiral Khan et al. (2013); Sobolenko et al. (2017); Khan et al. (2018).

The paper is structured as follows: in Section 1 we present the introduction to the topic; in Appendix A we describe the numerical method; in Section 2 we describe the system of units and initial conditions used in our N-body simulations; in Section 3 we describe the hardening rates found in our simulations for different binary SMBH mass ratios; whereas in Section 4 we summarize and discuss the main conclusions of our paper.

2. UNITS AND INITIAL CONDITIONS

We analyze a suite of 68 N-body simulations comprised of $N = 25k, 50k, 100k, 250k, 400k, 1M$ particles, modeling the evolution of an SMBHB embedded in a rotating galactic nucleus, to reproduce the typical environment of the inner regions of a post-merged galaxy. Details about these simulations are provided in Berczik et al. (2006) and Berentzen et al. (2009), whereas in this work we focus only on the analysis of their outcome. We briefly summarize the main features of our models as follows.

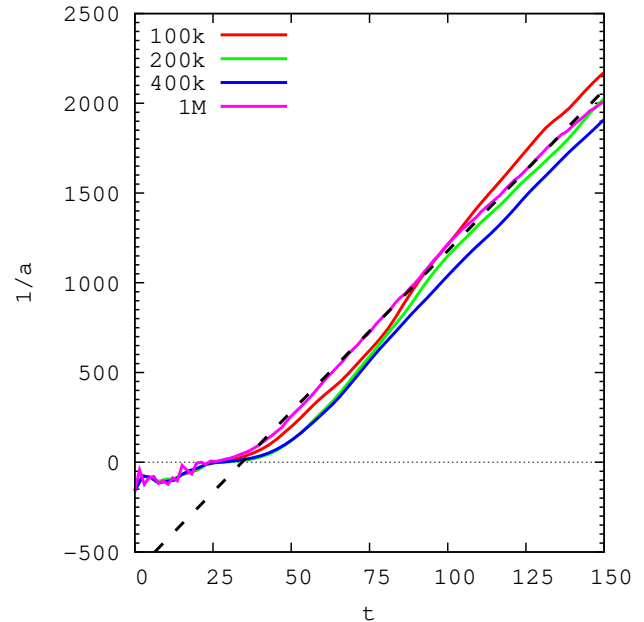


Figure 1. This figure shows the inverse of the binary’s semi-major axis a as a function of time for the four different particles numbers N (100k, 200k, 400k, 1M) model with SMBH mass ratio $m_1 : m_2 = 0.01 : 0.002$. The black dashed line shows the common corresponding linear fit between the time interval $t = 50 - 150$.

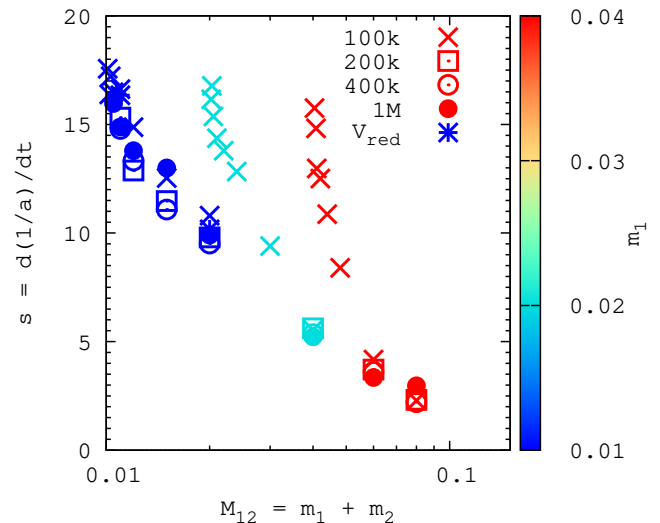


Figure 2. Hardening rate for SMBH binaries with different mass ratios $q = m_2/m_1$ (note $m_1 \geq m_2$) as a function of the binaries total mass $M_{12} = m_1 + m_2$. Different symbols represent models with different particle numbers N (see Table 1), respectively. The colors are used to indicate the primary SMBH mass m_1 .

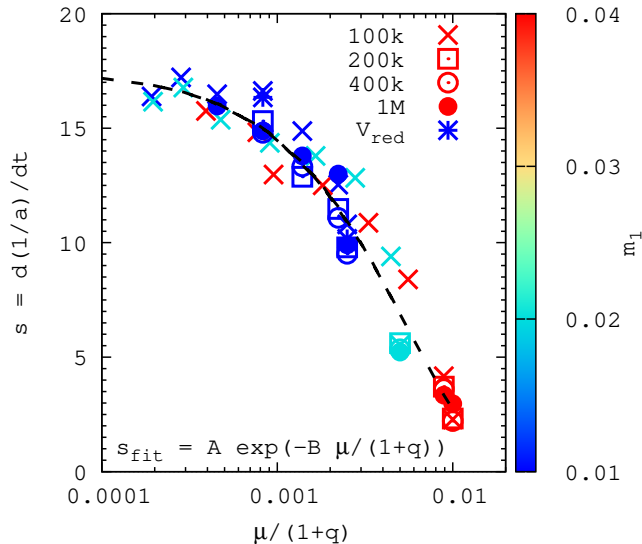


Figure 3. Hardening rate as a function of the ratio between the reduced mass and the mass ratio, $\mu/(1+q)$. Color coding marks the mass of the primary component, whereas different symbols refer to different models.

All simulations are initially scaled applying the standard strategy for N -body normalization (Aarseth et al. 1974), according to which both the gravitational constant and the total mass of the stellar system are set to unity, $G = M = 1$, and the total energy of the system is set to $E = -\frac{1}{4}$. The galactic nucleus follows initially a rotating King distribution function (see, e.g., Einsel & Spurzem 1999, and references therein). We set the dimensionless potential well (King parameter) and rotation parameters to $W_0 = 6$ and $\omega_0 = 1.8$, respectively, in all our models. At the center of the nucleus, we place two SMBHs initially unbound with primary mass $m_1 = (1 - 4) \times 10^{-2}$ times the nucleus mass and the mass ratio $q = 10^{-4} - 1$. The corresponding range of reduced mass adopted is thus $\mu \equiv m_2 \cdot m_1 / (m_1 + m_2) = 9.9 \times 10^{-3} - 2$. The total angular momentum vector of both the stellar nucleus and the SMBHs are aligned with the z -axis of our coordinate frame. We place the two SMBHs in the $z = 0$ mid-plane with initial coordinate components $x_{1,2} = 0$ and $y_{1,2} = \pm 0.3$, where the sub-scripts denotes the two SMBHs. Note that the SMBHs coordinates are given in N -body units, and the distance from the center of the SMBHs particles roughly corresponds to the influence radius of models in which the SMBHB has a total mass of 2×10^{-2} .

The initial velocities for the two SMBH is oriented along the x -axis and set to $v_{x;1,2} = \pm V_{\text{circ}}$, where V_{circ} is the circular velocity within the stellar background model. Note that our choice of initial parameter and scaling implies a circular velocity $V_{\text{circ}} \approx 0.7$ in N -body units, at the initial SMBH position.

We complement our simulations database with a extra set of 4 further models in which we assume for the SMBH initial velocity $v_{x;1,2} = \pm 0.1 V_{\text{circ}} \approx 0.07$. This choice implies that the SMBHs move initially on more eccentric orbits compared to the other simulations, thus allowing them to pair in a shorter timescale. All the main features of our models are summarized in Table 1.

3. RESULTS AND DISCUSSION

Due to the initial rotation, the stellar distribution undergoes bar-instability and form a rotating triaxial nucleus, as discussed in our previous works (Berczik et al. 2006; Berentzen et al. 2009). The two SMBHs migrate inward due to dynamical friction until to the point at which they become gravitationally bound.

After the SMBHB formation, continuous interactions with the surrounding field stars causes the shrinking of the orbit, i.e. a progressive decrease of the binary semi-major axis a . The semi-major axis evolution can be dissected in two phases, one during which the binary orbit evolution is driven by both dynamical friction and stellar hardening, and another, dominated by stellar encounters, during which the binary shrinking proceeds at a nearly constant rate.

Figure 1 shows the time evolution of the inverse of the binary semi-major axis ($1/a$) in the case of a set of models characterized by $m_1 : m_2 = 0.01 : 0.002$, assuming $N = 100k, 200k, 400k$ and $1M$. The plot outlines that the hardening follows a nearly linear trend, regardless of the number of particles. Therefore the slope of the $1/a$ curve provides us with an estimate of the binary hardening rate, $s(t) = d(1/a)/dt$. The black dashed line in Figure 1 represents the best-fitting linear relation calculated for the time interval $t = 50 - 150$ (N -body units). By definition, integrating over time the relation $s(t)$ would enable us to infer the binary evolution as consequence of stellar hardening. Coupling the hardening rate with the extra hardening triggered by GW emission enables to infer the binary merger time (e.g. Gualandris & Merritt 2012; Arca-Sedda & Gualandris 2018).

Figure 2 shows the dimensionless hardening rate for SMBHBs with different mass ratios $q \equiv m_2/m_1$ as a function of the binary total mass $M_{12} = m_1 + m_2$ for models with different particle numbers N (see Table 1) and different values of the mass of the primary SMBH. The plot outlines how, at a fixed SMBHB total mass, a heavier primary – i.e. a lower mass ratio – determines larger hardening. Similarly, at fixed primary mass, we see that heavier binaries – i.e. heavier companions – are associated with a smaller hardening rate. This implies that the efficiency of stellar hardening is maximized for low mass-ratio SMBHBs with a heavy primary mass. This result holds regardless of the number of particles used, thus confirming that is a physical effect rather than numerical.

Taking advantage of scattering experiments, Rasskazov et al. (2019) recently showed that for low

Table 1. Set of parameters of our model runs.

m_2	m_1	μ	025k	050k	100k	250k	400k	1M
10^{-2}	10^{-2}	10^{-2}						
0.01	1	0.0099	—	—	450	—	—	—
0.02	1	0.0196	—	—	450	—	—	—
0.03	1	0.0291	—	—	350	—	—	—
0.05	1	0.0476	—	—	350	—	—	—
0.10	1	0.0909	250	250	250*	250	250	150
0.20	1	0.1666	250	250	250*	250	250	150
0.50	1	0.3333	250	250	250*	250	250	150
1.00	1	0.5000	250	250	250*	250	250	150
0.02	2	0.0198	—	—	450	—	—	—
0.03	2	0.0295	—	—	450	—	—	—
0.05	2	0.0488	—	—	350	—	—	—
0.10	2	0.0952	—	—	350	—	—	—
0.20	2	0.1818	—	—	250	—	—	—
0.40	2	0.3333	—	—	250	—	—	—
1.00	2	0.6666	250	250	250	250	250	150
2.00	2	1.0000	250	250	250	250	250	150
0.04	4	0.0396	—	—	450	—	—	—
0.08	4	0.0784	—	—	450	—	—	—
0.10	4	0.0976	—	—	350	—	—	—
0.20	4	0.1905	—	—	350	—	—	—
0.40	4	0.3636	—	—	250	—	—	—
0.80	4	0.6666	—	—	250	—	—	—
2.00	4	1.3333	250	250	250	250	250	150
4.00	4	2.0000	250	250	250	250	250	150

NOTE—Col. 1-2: SMBH masses (primary and secondary correspondingly) in a 10^{-2} model units. Col. 3: reduced mass $\mu \equiv m_2 \cdot m_1 / (m_1 + m_2)$ in a 10^{-2} model units. Col. 4 – 9: Particle number in the stellar galactic nucleus. *: in these simulations we did two independent set of runs. After the first set of runs, where the initial orbital velocity of the SMBH was exactly circular V_{circ} , we run a second set of runs where the initial velocity of the SMBHs was $0.1 V_{\text{circ}}$.

mass ratios ($q < 10^{-2}$) the hardening rate is proportional to $(1 + q)^2 / q$. We find a similar dependence in our full N-body models, namely that the hardening is tightly described by a simple relation involving the primary mass and mass ratio:

$$\frac{(1 + q)^2}{q} \frac{1}{m_1} \equiv \frac{(1 + q)^2}{m_2} \equiv \frac{1 + q}{\mu}. \quad (1)$$

Figure 3, shows the relation between the hardening rate and the $\mu / (1 + q)$ quantity. We find that this relation is well fitted by the following simple exponential formula:

$$s = A \exp(-B\mu / (1 + q)), \quad (2)$$

with $A = 17.5 \pm 0.3$ and $B = 186 \pm 9$. Note that this relation implies that the secondary mass and the total mass ratio play the most effective role in shaping of the SMBHB evolution.

The fitting formula provided above enables to link the binary hardening rate to the masses of the binary components. Figure 3 compares our fitting formula with the simulated data for the 52 largest N models considered here. We see that passing from $\mu / (1 + q) = 10^{-4}$ to 10^{-2} the hardening rate decreases by a factor of 5. At a fixed primary mass, this implies that highly asymmetric binaries ($q \ll 1$) tend to be characterized by a more effective hardening compared to the case of nearly equal mass SMBHBs. This might crucially affect the merger efficiency of SMBH's in minor galaxy mergers, which are expected to contribute to the formation of SMBHB with mass ratio 1:10 - 1:3 especially at high redshift (e.g. Callegari et al. 2011). Primary mass values $10^6 - 10^7 M_{\odot}$ merging with a small companion might be bright GW sources for the laser interferometer space antenna (LISA Amaro-Seoane et al. 2017) and similar

space-based detectors like TianQin (Luo et al. 2016), Taiji (Ruan et al. 2018), or μ Ares (Sesana et al. 2019).

4. SUMMARY

We have presented a systematic study of the evolution of asymmetric SMBH binaries harbored in a non-axisymmetric, dense stellar galactic nucleus. To be able to perform this large systematic set of direct N -body simulations we have developed a new high-performance computing code φ -GPU that enables full exploiting of current and next generations high-performance GPU clusters.

Our simulations suggest that the binary hardening rate for unequal mass SMBHB does not depend on the number of particles N , at least in the regime investigated here. The stellar hardening in our modelled SMBHBs is sufficiently effective to drive the SMBHB toward coalescence in a short timescale \sim Gyr Berentzen et al. (2009).

For a fixed mass of the primary SMBH, i.e., the more massive one, we find an significant increase in the hardening rate for smaller masses of the secondary (i.e., lighter) SMBH. On the other hand, for a fixed mass of the secondary SMBH we find the hardening rate to be proportional to the primary’s mass.

We find a tight relation between the hardening rate and the binary total mass $M_{1,2}$ and reduced mass μ , which suggests that SMBHB shrinkage process can be described by a two-parameters relation. Smaller values of $M_{1,2}$ and μ result in an increase of the hardening rate. The hardening rates in our models support predictions of 3-body scatter experiments (see e.g., Hills & Fullerton 1980; Hills 1983; Rasskazov et al. 2019), which suggests a scaling between hardening rate and binary mass ratio.

ACKNOWLEDGMENTS

We thanks to our colleagues Andreas Just, Ingo Berentzen and Long Wang for their significant help and fruitful discussions during the preparation of the present work.

The work of PB, MAS, MS and MI was supported by the Deutsche Forschungsgemeinschaft (DFG, German Research Foundation) Project-ID 138713538, SFB 881 (“The Milky Way System”) and by the Volkswagen Foundation under the Trilateral Partnerships grant No. 97778.

PB acknowledges support by the Chinese Academy of Sciences (CAS) through the Silk Road Project at NAOAC, the Presidents International Fellowship (PIFI) for Visiting Scientists program of CAS and the National Science Foundation of China (NSFC) under grant No. 11673032.

MS acknowledges support by the National Academy of Sciences of Ukraine under the Research Laboratory Grant for young scientists No. 0120U100148. MS acknowledges support by Ministry of Education and Sci-

ence of Ukraine under the Fellowship of the President of Ukraine for young scientists. MS and MI acknowledges support by the National Academy of Sciences of Ukraine under the Research Project of young scientists No. 0119U102399.

The work of PB was also partially supported under the special program of the National Academy of Sciences of Ukraine “Support for the development of priority fields of scientific research” (CPCEL 6541230).

MAS acknowledges financial support from the Alexander von Humboldt Foundation for the research program “The evolution of black holes from stellar to galactic scales”.

APPENDIX

A. NUMERICAL METHOD

The simulations presented in this work have been carried out using the direct N -body code φ -GPU code. Our N -body package use a high order Hermite integration scheme and individual block time steps (the code supports time integration of particle orbits with 4th, 6th and even 8th order schemes). Such a direct N -body code evaluates in principle all pairwise forces between the gravitating particles, and its computational complexity scales asymptotically with N^2 . We refer the more interested readers to a general discussion about different N -body codes and their implementation in [Berczik et al. \(2011, 2013a\)](#).

The φ -GPU code is fully parallelized using the MPI library, This code is rewritten from scratch in C++ and based on earlier CPU serial N -body code (YEBISU; [Nitadori & Makino \(2008\)](#)). The MPI parallelization was done in the same “j” particle parallelization mode as in the earlier φ -GRAPE code ([Harfst et al. 2007](#)). All the particles are divided equally between the working nodes and in each node the fractional forces are calculated only for the so called “active” – “i” particles at the current time step. Due to the hierarchical block time step scheme the average number N_{act} of active particles (particles for which the forces are computed at a given time level) is usually small compared to the total particle number N , but it’s actual value can vary from 1 to N . The full forces from all of the particles acting on the active particles are obtained after using the global MPI communication routines.

The current version of the φ -GPU ¹ code uses a native GPU support and direct code access to the GPU using the NVIDIA native CUDA library. The multi GPU support is achieved through global MPI parallelization. Each MPI process uses only a single GPU, but usually up to four MPI processes per node are started (in order to effectively use the multi core CPUs and the multiple GPUs on our clusters). Simultaneously, our code effectively exploits also the current CPU’s OpenMP parallelization. Each MPI process on the nodes can uses up to 16 OMP cores in parallel (mainly for the loop parallelization in the C++ part of the main code). The code is designed to use different softening parameters for the gravity calculation (if it is required) for different astrophysical components in our simulations like SMBHs, dark matters or stars particles. More details about the φ -GPU code public version and its performance we are presented in [Berczik et al. \(2011, 2013a\)](#). The present code is well tested and already used to obtain important results in our earlier large scale (up to few million body) simulations ([Kennedy et al. 2016; Wang et al. 2014; Zhong et al. 2014; Li et al. 2012; Just et al. 2012](#)).

Before we start our production runs for the different particles number we first check the optimal integration parameter η which controls the accuracy of the integration. For this reason we start the $N=8k$ model with 6 different values of $\eta = 0.020, 0.010, 0.007, 0.005, 0.002, 0.001$. The time steps we are calculated using the standard Aarseth timestep criteria ([Aarseth 1985](#)).

After the total energy check we see that the optimal η parameter (speed vs. accuracy) is around 0.01. The total energy drift (dE_{tot}/dt) for this range of η in our simulation is vary from $5 \cdot 10^{-9}$ to $2 \cdot 10^{-12}$. With such a integration parameter our largest the $N=1M$ particle simulation up to $t_{\text{end}} = 150$ on our GPU computing system (with NVIDIA K20 GPU) take ~ 140 hours of real computation time with the total code performance around ~ 1.15 Gflops.

REFERENCES

- Aarseth, S. J. 1985, in Multiple time scales, 377–418
- Aarseth, S. J., Henon, M., & Wielen, R. 1974, *A&A*, 37, 183
- Amaro-Seoane, P., Aoudia, S., Babak, S., et al. 2013, *GW Notes*, 6, 4. <https://arxiv.org/abs/1201.3621>
- Amaro-Seoane, P., Audley, H., Babak, S., et al. 2017, arXiv e-prints, arXiv:1702.00786. <https://arxiv.org/abs/1702.00786>
- Arca-Sedda, M., & Gualandris, A. 2018, *MNRAS*, 477, 4423, doi: [10.1093/mnras/sty922](https://doi.org/10.1093/mnras/sty922)
- Begelman, M. C., Blandford, R. D., & Rees, M. J. 1980, *Nature*, 287, 307, doi: [10.1038/287307a0](https://doi.org/10.1038/287307a0)
- Berczik, P., Merritt, D., Spurzem, R., & Bischof, H.-P. 2006, *ApJL*, 642, L21, doi: [10.1086/504426](https://doi.org/10.1086/504426)
- Berczik, P., Spurzem, R., & Wang, L. 2013a, in Third International Conference “High Performance Computing”, HPC-UA 2013, p. 52-59, 52–59. <https://arxiv.org/abs/1312.1789>
- Berczik, P., Spurzem, R., Zhong, S., et al. 2013b, in Lecture Notes in Computer Science, Vol. 7905, Procs. of 28th Intl. Supercomputing Conf. ISC 2013, Leipzig, Germany, June 16-20, 2013., ed. J. M. Kunkel, T. Ludwig, & H. E. Meuer (Springer Vlg.), 13–25
- ¹ <ftp://ftp.mao.kiev.ua/pub/berczik/phi-GPU/>

- Berczik, P., Nitadori, K., Zhong, S., et al. 2011, in International conference on High Performance Computing, Kyiv, Ukraine, October 8-10, 2011., p. 8-18, 8-18
- Berentzen, I., Preto, M., Berczik, P., Merritt, D., & Spurzem, R. 2009, *ApJ*, 695, 455, doi: [10.1088/0004-637X/695/1/455](https://doi.org/10.1088/0004-637X/695/1/455)
- Callegari, S., Kazantzidis, S., Mayer, L., et al. 2011, *ApJ*, 729, 85, doi: [10.1088/0004-637X/729/2/85](https://doi.org/10.1088/0004-637X/729/2/85)
- Einsel, C., & Spurzem, R. 1999, *MNRAS*, 302, 81, doi: [10.1046/j.1365-8711.1999.02083.x](https://doi.org/10.1046/j.1365-8711.1999.02083.x)
- Gong, X., Xu, S., Bai, S., et al. 2011, *Classical and Quantum Gravity*, 28, 094012, doi: [10.1088/0264-9381/28/9/094012](https://doi.org/10.1088/0264-9381/28/9/094012)
- Gualandris, A., & Merritt, D. 2012, *ApJ*, 744, 74, doi: [10.1088/0004-637X/744/1/74](https://doi.org/10.1088/0004-637X/744/1/74)
- Gültekin, K., Richstone, D. O., Gebhardt, K., et al. 2009, *ApJ*, 698, 198, doi: [10.1088/0004-637X/698/1/198](https://doi.org/10.1088/0004-637X/698/1/198)
- Harfst, S., Gualandris, A., Merritt, D., et al. 2007, *NewA*, 12, 357, doi: [10.1016/j.newast.2006.11.003](https://doi.org/10.1016/j.newast.2006.11.003)
- Hills, J. G. 1983, *AJ*, 88, 1269, doi: [10.1086/113418](https://doi.org/10.1086/113418)
- Hills, J. G., & Fullerton, L. W. 1980, *AJ*, 85, 1281, doi: [10.1086/112798](https://doi.org/10.1086/112798)
- Ho, L. C., & Kim, M. 2014, *ApJ*, 789, 17, doi: [10.1088/0004-637X/789/1/17](https://doi.org/10.1088/0004-637X/789/1/17)
- Just, A., Yurin, D., Makukov, M., et al. 2012, *ApJ*, 758, 51, doi: [10.1088/0004-637X/758/1/51](https://doi.org/10.1088/0004-637X/758/1/51)
- Kennedy, G. F., Meiron, Y., Shukirgaliyev, B., et al. 2016, *MNRAS*, 460, 240, doi: [10.1093/mnras/stw908](https://doi.org/10.1093/mnras/stw908)
- Khan, F. M., Capelo, P. R., Mayer, L., & Berczik, P. 2018, *ApJ*, 868, 97, doi: [10.3847/1538-4357/aae77b](https://doi.org/10.3847/1538-4357/aae77b)
- Khan, F. M., Fiacconi, D., Mayer, L., Berczik, P., & Just, A. 2016, *ApJ*, 828, 73, doi: [10.3847/0004-637X/828/2/73](https://doi.org/10.3847/0004-637X/828/2/73)
- Khan, F. M., Holley-Bockelmann, K., Berczik, P., & Just, A. 2013, *ApJ*, 773, 100, doi: [10.1088/0004-637X/773/2/100](https://doi.org/10.1088/0004-637X/773/2/100)
- Komossa, S. 2006, *Mem. Soc. Astron. Italiana*, 77, 733
- Li, S., Liu, F. K., Berczik, P., Chen, X., & Spurzem, R. 2012, *ApJ*, 748, 65, doi: [10.1088/0004-637X/748/1/65](https://doi.org/10.1088/0004-637X/748/1/65)
- Luo, J., Chen, L.-S., Duan, H.-Z., et al. 2016, *Classical and Quantum Gravity*, 33, 035010, doi: [10.1088/0264-9381/33/3/035010](https://doi.org/10.1088/0264-9381/33/3/035010)
- Naab, T., Jesseit, R., & Burkert, A. 2006, *MNRAS*, 372, 839, doi: [10.1111/j.1365-2966.2006.10902.x](https://doi.org/10.1111/j.1365-2966.2006.10902.x)
- Naab, T., Johansson, P. H., & Ostriker, J. P. 2009, *ApJL*, 699, L178, doi: [10.1088/0004-637X/699/2/L178](https://doi.org/10.1088/0004-637X/699/2/L178)
- Nitadori, K., & Makino, J. 2008, *NewA*, 13, 498, doi: [10.1016/j.newast.2008.01.010](https://doi.org/10.1016/j.newast.2008.01.010)
- Rasskazov, A., Fragione, G., Leigh, N. W. C., et al. 2019, *ApJ*, 878, 17, doi: [10.3847/1538-4357/ab1c5d](https://doi.org/10.3847/1538-4357/ab1c5d)
- Rodriguez, C., Taylor, G. B., Zavala, R. T., et al. 2006, *ApJ*, 646, 49, doi: [10.1086/504825](https://doi.org/10.1086/504825)
- Ruan, W.-H., Guo, Z.-K., Cai, R.-G., & Zhang, Y.-Z. 2018, *arXiv e-prints*, arXiv:1807.09495, <https://arxiv.org/abs/1807.09495>
- Sesana, A., Korsakova, N., Arca Sedda, M., et al. 2019, *arXiv e-prints*, arXiv:1908.11391, <https://arxiv.org/abs/1908.11391>
- Sobolenko, M., Berczik, P., Spurzem, R., & Kupi, G. 2017, *Kinematics and Physics of Celestial Bodies*, 33, 21
- Valtonen, M. J. 2007, *ApJ*, 659, 1074, doi: [10.1086/512801](https://doi.org/10.1086/512801)
- Valtonen, M. J., Mikkola, S., Lehto, H. J., et al. 2010a, *Celestial Mechanics and Dynamical Astronomy*, 106, 235, doi: [10.1007/s10569-009-9252-z](https://doi.org/10.1007/s10569-009-9252-z)
- Valtonen, M. J., Mikkola, S., Merritt, D., et al. 2010b, *ApJ*, 709, 725, doi: [10.1088/0004-637X/709/2/725](https://doi.org/10.1088/0004-637X/709/2/725)
- Wang, L., Berczik, P., Spurzem, R., & Kouwenhoven, M. B. N. 2014, *ApJ*, 780, 164, doi: [10.1088/0004-637X/780/2/164](https://doi.org/10.1088/0004-637X/780/2/164)
- Zhong, S., Berczik, P., & Spurzem, R. 2014, *ApJ*, 792, 137, doi: [10.1088/0004-637X/792/2/137](https://doi.org/10.1088/0004-637X/792/2/137)